A Stochastic Model of Leukocyte Rolling

Yihua Zhao, Shu Chien, and Richard Skalak
Department of Bioengineering, University of California, San Diego, La Jolla, California 92093 USA

ABSTRACT Selectin-mediated leukocyte rolling under flow is an important process in leukocyte recruitment during inflammation. The rolling motion of individual cells has been observed to fluctuate randomly both in vivo and in vitro. This paper presents a stochastic model of the micromechanics of cell rolling and provides an analytical method of treating experimental data. For a homogeneous cell population, the velocity distribution is obtained in an analytical form, which is in good agreement with experimentally determined velocity histograms obtained previously. For a heterogeneous cell population, the model provides a simple, analytical method of separating the contributions of temporal fluctuations and population heterogeneity to the variance of measured rolling velocities. The model also links the mean and variance of rolling velocities to the molecular events underlying the observed cellular motion, allowing characterization of the distribution and release rate of the clusters of molecular bonds that tether the cell to substratum. Applying the model to the analysis of data obtained for neutrophils rolling on an E-selectin-coated surface at a wall shear stress of 1.2 dyn/cm^2 yields estimations of the average distance between bond clusters (~0.5 μm) and the average time duration of a bond cluster resisting the applied fluid force (~0.5 s).

INTRODUCTION

Adhesive interaction between leukocytes and the endothelial lining of blood vessels is a hallmark of acute inflammation, both as a physiological response to tissue injury and infection, and as a pathological condition such as found in myocardial infarction, acute lung failure, and vasculitis. In a rare hereditary disease called leukocyte adhesion deficiency (LAD), the congenital absence or defect of certain types of adhesion molecules on neutrophil surfaces reduces neutrophil adhesion and chemotaxis and thus results in inadequate host defense (von Andrian et al., 1993; Harlan, 1993; Etzioni et al., 1993). On the other hand, antiadhesion has become the central idea in many efforts to develop new drugs treating inflammatory diseases (Welply et al., 1994).

The adhesive interaction between leukocytes and endothelial cells occurs in the face of the dislodging hemodynamic forces exerted on the adhering leukocytes by the blood flow. The initial step of interaction with the endothelium during inflammatory response occurs when leukocytes roll along the stimulated endothelial cells in postcapillary venules (Fiebig et al., 1991; von Andrian et al., 1991; Ley, 1993). This rolling is mediated by adhesion molecules belonging to the selectin family (von Andrian et al., 1991; Ley, 1993; McEver, 1994). During rolling, the leukocytes may also be stimulated, and consequently another family of cell adhesion molecules, the integrins, is activated on the leukocyte surface. The integrins mediate the firm adhesion and spreading of the leukocytes onto the endothelium, followed by their extravasation into the infected tissues (Lorant et al., 1993). The findings that rolling and firm adhesion are mediated by cell adhesion molecules from different families have generated intensive research interests in recent years, including investigation of the physical and chemical factors that enable selectins to arrest fast-moving leukocytes and produce the rolling process. Selectins have been extensively investigated since their identification in the 1980s. L-, E-, and P-selectins are monomeric linear transmembrane glycoproteins, closely related to each other in primary structure. Each of them contains an N-terminal domain, which is related to those in Ca^{2+}-dependent lectins and is directly involved in cell-cell adhesion by interacting with cell surface carbohydrate ligands. L-selectin is constitutively presented on the leukocyte surface; E-selectin is induced on cytokine-stimulated endothelial cells; and P-selectin is expressed by thrombin- or histamine-stimulated endothelial cells and platelets (for reviews, see Springer, 1990; Lasky, 1992; Bevilacqua and Nelson, 1993; McEver, 1994).

Leukocyte rolling can be observed in vivo by intravital microscopy and in vitro in flow chambers, in which isolated leukocytes are rolling on either monolayers of cultured endothelial cells or surfaces coated with selectin or other molecules. The velocities of rolling cells are usually orders of magnitude slower than the velocities of nonadherent cells freely moving close to the substratum surface, indicating adhesive interaction between the rolling cells and the substratum (Lawrence and Springer, 1991; Ley, 1993). It has been shown that both P- and E-selectins can mediate neutrophil rolling (Lawrence and Springer, 1991, 1993; Jones et al., 1993; Abbassi et al., 1993), but the resulting rolling behaviors are somewhat different. Under comparable experimental conditions, the velocity of neutrophil rolling on E-selectin is slower. Furthermore, there is a difference in the dependence of average rolling velocities on wall shear

Received for publication 27 December 1994 and in final form 23 June 1995.

Address reprint requests to Dr. Richard Skalak, Department of Bioengineering, University of California, San Diego, 9500 Gilman Dr., Department 0412, La Jolla, CA 92093. Tel.: 619-534-5119; Fax: 619-534-8908; E-mail:rskalak@ames.ucsd.edu.

0006-3495/95/10/1309/12 $2.00

stress. For P-selectin, the velocity increases with increasing wall shear stress (from <1 to 8 dyn/cm^2) (Lawrence and Springer, 1991; Jones et al., 1993), but for E-selectin the velocity appears to reach a plateau level, which is a function of E-selectin density (Lawrence and Springer, 1993).

The motion of leukocyte rolling has been observed to have some stochastic or random features both in vivo (Schmid-Schönbein et al., 1987) and in vitro (Goetz et al., 1994). The irregular motion has been referred to as saltation (Lipowsky et al., 1991), a term suggesting a stop-and-go pattern of the leukocyte motion. Variation of the rolling velocities of individual cells in time has also been mentioned for experiments in which the leukocytes roll on a flat surface bearing a uniform layer of ligands, either P- or E-selectins (Lawrence and Springer, 1991; 1993). This suggests that the fluctuation in rolling velocities is a reflection of the stochastic nature of the adhesive interaction. Neutrophils have microvilli that are not distributed uniformly, and their spacing has a certain degree of randomness. In unstimulated neutrophils, L-selectin is concentrated at the tips of microvilli (Picker et al., 1991; Erlandsen et al., 1993; Borregaard et al., 1994) and may present carbohydrate ligands to P- and E-selectins (Picker et al., 1991; Lawrence and Springer, 1993). It has been found that "neutrophil rolling was much steadier on E-selectin than on P-selectin, i.e., there was less variance over time in the velocity of individual cells" (Lawrence and Springer, 1993). Thus, as pointed out by Goetz et al. (1994), the dynamics of leukocyte rolling is not fully characterized by measurements of the average velocity alone.

Hammer and Apte (1992) developed a numerical method that simulates the interaction of a single cell with a ligand-coated surface under flow. The simulation generates statistical fluctuations in cellular motion by taking account of the statistical fluctuations in the spacing and numbers of binding molecules. They found that the mode of cellular motion is critically modulated by the constitutive relationship between the stretch of a bond and its rate of breakage. A limitation of this approach, as pointed out by the authors, is that the simulations are too lengthy to rapidly obtain information about the adhesive behavior of an ensemble of cells.

Tözeren and Ley (1992) introduced a quantitative biophysical model of leukocyte rolling. Their computational experiments indicate that selectins mediate leukocyte rolling with a mechanism in which the bond formation rate is high and the detachment rate is low, except at the rear of the contact area, where the stretched bonds detach at a uniform, high rate. Their model is deterministic, so only mean rolling velocities are derived and fluctuations of the rolling velocities are not treated.

The aims of the present paper are to develop a stochastic model for the random motion of rolling cells, to elucidate the micromechanics of leukocyte rolling, and to develop a simple, analytical method of extracting information from experimental data relevant to the molecular events underlying the cellular motion. Such information is buried in the variation of rolling velocities from time to time and from cell to cell, as well as in the average velocity.

GENERAL CONSIDERATIONS

In experiments on leukocytes viewed by light microscopy, it is regularly observed that rolling cells move in a stop-and-go pattern. This pattern of motion suggests an approximation of the displacement of the cell center as a stepwise function of time by a series of rapid steps in between which the cell velocity is zero. This is shown schematically in Fig. 2, where x is the instantaneous position of the cell centroid measured along the direction of the flow. This stepping phenomenon is a reflection of the molecular patchiness and the discrete nature of the adhesive interaction as described in the following micromechanical analysis of the rolling process.

As pointed out by Hammer and Apte (1992), only the adhesion molecules located on the tips of microvilli are accessible to their ligands (Fig. 1). Thus, the effective molecular bonds are clustered on the tips of microvilli. A step displacement occurs when the bonds on the rearmost microvillus are released. Between such events, the cell is essentially at rest and the remaining bonds must provide forces and torques that balance the hydrodynamic stresses exerted on a stationary cell by the imposed viscous flow. At the moment of release of one cluster of molecular bonds, the forces and torques of the adhesive interaction go through decremental changes. The hydrodynamic stresses acting on the cell surface then drive the cell forward rapidly to a new position, where a balance between the adhesive and hydro-

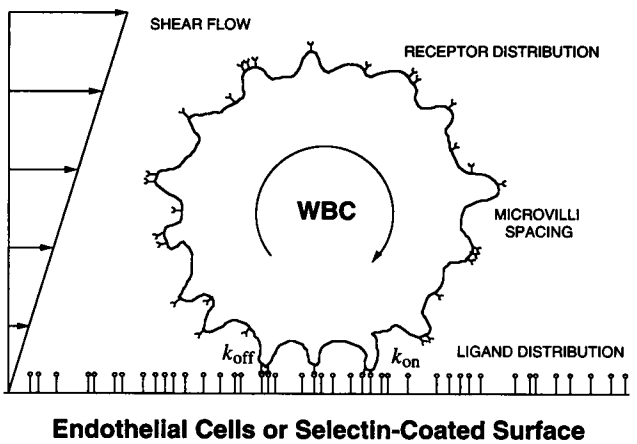

FIGURE 1 A schematic of the model for a rolling leukocyte. The cell is tethered to the substratum by receptor-ligand bonds, which are clustered at the tips of microvilli. The fluid drag on the cell stretches the bonds at the rearmost microvillus, thus increasing their effective dissociation rate k_{off}. When the rearmost microvillus is released, the cell is driven forward rapidly by the fluid flow to a new position, with a random stepsize determined by the microvilli spacing, receptor and ligand distributions, and their association rate k_{on} at the leading edge of the contact zone. The random time interval between successive steps (waiting time) relates to the number and the dissociation rate of the stressed bonds at the rearmost microvillus as well as the applied stresses.

dynamic stresses on a stationary cell is reestablished. The resulting displacement h (step size) is a random variable determined mainly by the spacing of microvilli and by the distributions of adhesion molecules on the individual microvilli and the ligands on the substratum surface. The time duration of this displacement is

$$t_1 \sim \frac{h}{v_{\text{free}}}, \tag{1}$$

where v_{free} is the velocity of a free-flowing, nonadherent leukocyte. Let t_2 be the time interval between two successive events of the release of bond clusters. Then,

$$t_2 \sim \frac{h}{v_{\text{rolling}}}, \tag{2}$$

where v_{rolling} is the long-term average of the velocity of a rolling cell. Both t_1 and t_2 are considered to be random variables, as is the step size h. The physical origins of these random variables are shown schematically in Fig. 2. Denote the averages of t_1 and t_2 as τ_1 and τ_2, respectively. Then τ_1 is the average duration of a nonzero velocity period, and τ_2 is the average waiting time at zero velocity. These are the two characteristic intrinsic time scales that play important roles in the mechanics of cell rolling. From Eqs. 1 and 2, it follows that

$$\frac{\tau_1}{\tau_2} \sim \frac{v_{\text{rolling}}}{v_{\text{free}}}. \tag{3}$$

Experimental data show $(v_{\text{rolling}}/v_{\text{free}}) \ll 1$. Therefore, $\tau_1 \ll \tau_2$. This characterizes the cell motion in a stop-and-go pattern. Of course, when the step size h and/or the waiting time τ_2 are physically very small, detecting such a pattern may require temporal-spatial resolutions that are beyond the usual equipment limits. But, whenever $\tau_1 \ll \tau_2$, the microscopic picture of cell rolling can be idealized as being composed of random jumps whether we can readily measure the individual steps directly or not.

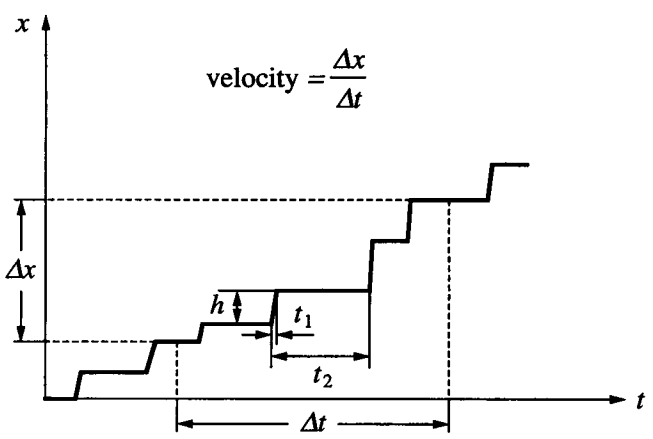

FIGURE 2 A schematic showing the idealized trajectory of a rolling cell. The cell position x is approximately a stepwise function of time, with random stepsize h and waiting time t_2. The time duration of stepping t_1 is much shorter than t_2. Rolling velocity is computed from the displacement Δx over a time window Δt, which is greater than t_2.

Monomeric soluble P-selectin binds to ~25,000 sites/neutrophil (Ushiyama et al., 1993). Assuming that these binding sites are concentrated on the tips of microvilli and that there are 6,000 microvilli/cell (Hammer and Apte, 1992), the average number of binding sites per microvillus is ~4. At high surface density of P-selectin or other adhesion molecules on the substratum, it is expected that there are usually more than one cluster of bonds tethering the cell to the substratum. However, because of the fact that the line of application of the resultant hydrodynamic force is above the cell-substratum interface (by ~1.4 cell radius), the bonds in the rearmost cluster are subject to tensile stresses. The tensile stresses on these bonds are expected to accelerate their dissociation rate. When the rearmost cluster of bonds is released under the influence of the hydrodynamic force, the remaining bond clusters will still tether the cell to the substratum. This prevents the cell from sliding. The cell rolls until the bonds in the rearmost remaining clusters are stretched and develop tensile stresses great enough to balance the hydrodynamic stresses. The motion of the cell is then rolling in small steps without sliding. This model is consistent with the reports of experimental observation that cells roll rather than slide both in vivo (Tözeren and Ley, 1992) and in vitro (Lawrence and Springer, 1991).

The waiting time t_2 is determined by the dissociation rate (and the number) of the mechanically stressed bonds in the rearmost clusters. If every cluster contains only a single bond (which can be a good approximation when the surface density of ligands on the substratum is low), t_2 is precisely the lifetime of a stressed bond. If it is further assumed that the receptor-ligand bonds have a first order dissociation kinetics, the inverse of the average waiting time will give us the dissociation rate constant, i.e., $k_{\text{off}} = 1/\tau_2$. This points to a way to experimentally determine k_{off} of the adhesion bonds involved in cell rolling as a function of the mechanical force applied to the bonds, provided that there is a method to estimate τ_2 from the data of cell rolling, which is presented in this paper. For the cases of multiple-bond clusters, k_{off} and $1/\tau_2$ are functions of the applied forces on the bonds, but the precise relationship will be more complicated.

The step size h provides information about the spatial distribution of adhesion receptors and ligands. When the surface density of ligands on substratum is high and homogeneous, h indicates the spatial distribution of the clusters of adhesion receptors on the cell surface, i.e., essentially the microvilli spacing.

The hypothesis that at a microscopic level a rolling cell moves at a stop-and-go pattern allows us to define the waiting time t_2 and step size h as the intermediate variables linking the observable quantities at the cellular level to the underlying events at the molecular scale. The question treated herein is how to estimate t_2 and h from the measured distribution of cellular rolling velocities.

STOCHASTIC MODEL OF CELL ROLLING FOR A HOMOGENEOUS POPULATION

Here we consider a homogeneous population of leukocytes as an ensemble of identical cells. The stationary distribution of rolling velocities is considered for such an ensemble, and the parameters in the distribution function are related to the underlying molecular events. This is done based on the observation that the instantaneous displacement of a given cell is a stepping process with random jumps at random times (Fig. 2). Smoothing this stepping process by taking the moving average of the process over a time window Δt ($\Delta t \gg \tau_2$) makes it possible to model the cell velocity as a diffusion process; i.e., the evolution of the cell velocity is governed by a Fokker-Planck equation. The drift and diffusion coefficients in the Fokker-Planck equation are derived from the nonsmoothed stepping process of cell displacement and expressed in terms of the step size and waiting time of this stepping process. Integrating the stationary Fokker-Planck equation yields the theoretical distribution of velocity as a function of the step size h and waiting time τ_2 intrinsic to the rolling process, as well as the time window Δt chosen by the experimenter to analyze the process.

Fokker-Planck equation for the evolution of velocity distribution

The choice of the time window Δt is influenced by various experimental conditions such as the temporal-spatial resolutions of the equipment, the average velocity of the rolling cells, and the convenience of data acquisition and analysis. The usual values of Δt range from 1 to 20 s, which are generally greater than τ_2 and thus much greater than τ_1. It is clear that the experimentally determined velocity cannot be considered to be the instantaneous velocity of the cell. In accordance with the usual experimental method, we define the cell velocity as

$$v(t) \equiv \frac{x(t + \tfrac{1}{2}\Delta t) - x(t - \tfrac{1}{2}\Delta t)}{\Delta t}, \tag{4}$$

which can be shown to be the moving average of the instantaneous velocity dx/dt. In Eq. 4 $x(t)$ is the instantaneous position of the cell at time t.

It can be seen that $v(t)$ given by Eq. 4 is also a stepping process. When $\Delta t/\tau_2$ is large enough, the individual jumps of $v(t)$ are small and $v(t)$ is approximately continuous. In such a case, the stochastic process $v(t)$ can be modeled as a diffusion process, i.e., the evolution of the velocity distribution obeys a Fokker-Planck equation

$$\frac{\partial p(v,t)}{\partial t} = -\frac{\partial}{\partial v}[A(v)\,p(v,t)] + \frac{1}{2}\frac{\partial^2}{\partial v^2}[B(v)\,p(v,t)], \tag{5}$$

where $p(v, t)$ is the probability density of the moving-averaged velocity v at time t, and A and B are the drift and diffusion coefficients, respectively.

In the following, $\langle\ \rangle$ always denotes ensemble average. The drift coefficient in Eq. 5 is the derivative of the first transition moment of the random process v:

$$A(v) = \lim_{t' \to t} \frac{\langle v' - v \rangle}{t' - t}, \tag{6}$$

where v' is a realization of the random process at time $t' > t$, given the condition that the realization of the process at time t is v. Substituting the velocity definition Eq. 4 into Eq. 6 and rearranging, the resultant equation yields

$$A(v) = \lim_{t' \to t} \frac{\langle x(t' + \tfrac{1}{2}\Delta t) - x(t + \tfrac{1}{2}\Delta t)\rangle - \langle x(t' - \tfrac{1}{2}\Delta t) - x(t - \tfrac{1}{2}\Delta t)\rangle}{(t' - t)\Delta t}. \tag{7}$$

Note that the quantities under the two ensemble-average operators are the cell displacements over time duration $\delta t = t' - t$ at the two end moments of the time window Δt.

Let the mean and variance of the step size of jumps h (ensemble averages) be, respectively,

$$\bar{h} \equiv \langle h \rangle, \qquad \sigma_h^2 \equiv \langle (h - \bar{h})^2 \rangle. \tag{8}$$

When $\delta t \ll t_2$, we have

$$\langle x(t + \delta t) - x(t) \rangle = \left\langle h \cdot \left[\frac{\delta t}{\langle t_2 \rangle} + o(\delta t) \right] \right\rangle, \tag{9}$$

where it is assumed that the probability of a jump during δt is $[\delta t/\langle t_2 \rangle] + o(\delta t)$. Now, consider $\langle t_2 \rangle$, the ensemble average of the time interval between successive jumps. If no condition is imposed, $\langle t_2 \rangle$ is simply the waiting time τ_2 defined previously. However, when δt is a part of time interval $[t - \Delta t/2, t + \Delta t/2]$ and the moving-averaged velocity v at time t is specified, we have $\langle t_2 \rangle = \bar{h}/v$.

In Eq. 7, the first ensemble average is not conditioned, whereas the second ensemble average is conditioned with the specification of v at time t. Calculating the right-hand side of Eq. 7 according to the above discussion yields

$$A(v) = \frac{(\bar{v} - v)}{\Delta t}, \tag{10}$$

where

$$\bar{v} = \frac{\bar{h}}{\tau_2}, \tag{11}$$

which, with the use of ergodic assumption, can be shown to be the stationary ensemble average of the rolling velocities.

The diffusion coefficient B in Eq. 5 quantifies the rate of the dispersion of rolling velocities in the v-space due to the random fluctuation in the velocity of individual cells. It can

be computed from the second transition moment of the random process v:

$$B(v) = \lim_{t' \to t} \frac{\langle (v' - v)^2 \rangle}{t' - t}, \tag{12}$$

where v' is again the cell velocity at time $t' > t$, given the condition that the cell velocity at time t is v. Using Eq. 4, this diffusion coefficient can be found to be

$$B(v) = \lim_{t' \to t} \frac{\langle \{[x(t' + \frac{1}{2}\Delta t) - x(t + \frac{1}{2}\Delta t)] - [x(t' - \frac{1}{2}\Delta t) - x(t - \frac{1}{2}\Delta t)]\}^2 \rangle}{(t' - t)(\Delta t)^2}.$$

where, as in Eq. 7, the two square brackets are the cell displacements over the time duration $\delta t = t' - t$ at the two end moments of the time window Δt. When $\delta t \ll t_2 < \Delta t$, we expect that the two square brackets are statistically independent. Then,

$$B(v) = \frac{1}{(\Delta t)^2} \lim_{t' \to t} \frac{\langle [x(t' + \frac{1}{2}\Delta t) - x(t + \frac{1}{2}\Delta t)]^2 \rangle + \langle [x(t' - \frac{1}{2}\Delta t) - x(t - \frac{1}{2}\Delta t)]^2 \rangle}{t' - t}. \tag{13}$$

As in Eq. 7, the second ensemble average is conditioned with a known velocity v (averaged over Δt). The first ensemble average, however, needs further examination. Because the diffusion coefficient is a measure for the rate of the velocity dispersion due to random fluctuations, all of the systematic bias must be excluded in computing the second transition moment of the velocity using Eq. 13. As demonstrated in the derivation of the drift coefficient Eq. 10, the relaxation of the constrictive condition imposed on the velocity is the systematic bias from which the drift term in Eq. 5 arises. Therefore, to exclude the systematic bias, we need to keep the first ensemble average in Eq. 13 conditioned with the known velocity v (average over Δt). Then the two ensemble averages in Eq. 13 are equal. With an approach similar to the one used in deriving the drift coefficient Eq. 10, we obtain from Eq. 13

$$B(v) = \frac{2\langle h^2 \rangle}{\bar{h}(\Delta t)^2} \cdot v = \frac{2\bar{h}}{(\Delta t)^2}\left(1 + \frac{\sigma_h^2}{\bar{h}^2}\right) \cdot v. \tag{14}$$

The proportionality of the diffusion coefficient B to the rolling velocity v reflects the fact that the faster a cell moves, the more frequently its microvilli adhere and debond. Inserting Eqs. 10 and 14 into Eq. 5 and multiplying the two sides by Δt result in

$$\Delta t \frac{\partial p(v, t)}{\partial t} = \frac{\partial}{\partial v}[(v - \bar{v})\, p(v, t)] + \frac{\partial^2}{\partial v^2}\left[\frac{\bar{h}}{\Delta t}\left(1 + \frac{\sigma_h^2}{\bar{h}^2}\right) v p(v, t)\right]. \tag{15}$$

This is the Fokker-Planck equation that governs the time evolution of the velocity distribution $p(v, t)$, with the drift and diffusion coefficients given in terms of the variables $\bar{h}$, σ_h^2, and τ_2. It is anticipated that τ_2 will be inversely related to the dissociation rate of molecular bonds under stress.

Boundary conditions for the Fokker-Planck equation

A flux of probability flow can be defined in the v-space

$$J(v, t) = -\frac{v - \bar{v}}{\Delta t} p(v, t) - \frac{\partial}{\partial v}\left[\frac{\bar{h}}{(\Delta t)^2}\left(1 + \frac{\sigma_h^2}{\bar{h}^2}\right) v p(v, t)\right]. \tag{16}$$

This is similar to probability flux in statistical gas dynamics theory considering particle velocities and other physical cases. The Fokker-Planck equation (Eq. 15) states the conservation of probability mass, i.e., the time derivative of the probability density $p(v, t)$ equals the negative divergence of the probability flux $J(v, t)$.

The velocity of a rolling cell is restricted (i.e., $v \geq 0$) because of the imposed shear flow. Inserting Eq. 11 into Eq. 16 and evaluating the probability flux at the boundary $v = 0$ yields $J(0, t) \geq 0$, provided that $\Delta t \geq \tau_2(1 + \sigma_h^2/\bar{h}^2)$, which is a requirement consistent with the condition on the window size Δt for the moving averaging introduced at the beginning and is necessary for the time-averaged velocity $v(t)$ to be smooth enough to be appropriately described as a diffusion process. The inequality $J(0, t) \geq 0$ indicates that the probability flow is carried into the region of positive velocity through the boundary $v = 0$. Because for cell rolling there is no source of probability to the left of $v = 0$, the probability flow must vanish at this boundary, i.e.,

$$J(0, t) = 0. \tag{17}$$

This states that there is a natural reflecting boundary at $v = 0$.

Let v_m denote the upper boundary for the rolling velocities. Assuming that there is no source of probability introduced by external agents within the region $(0, v_m)$, the probability flow at the boundary $v = v_m$ must vanish also because the total probability mass is conserved. This second boundary condition can be replaced by, and is equivalent to, the normalization condition on $p(v, t)$, i.e., the integral of $p(v, t)$ with respect to v over $[0, v_m]$ must be unity. The value of v_m may be prescribed by physical reasoning. But for cell rolling such a prescription is subject to ambiguity. Hence, for the model to be appropriate, the dependence of its solution on the numerical value of v_m should be vanishingly weak to ensure the stability of the solution with respect to the disturbance in boundary conditions. It is expected that most probability mass is concentrated around the mean, which is far away from the upper bound of the possible rolling velocities v_m. Furthermore, the effect of v_m on the velocity distribution from the model is restricted to its appearance in the normalization of $p(v, t)$ as the upper limit of integration. Therefore, v_m can be set equal to infinity.

This will be justified by posterior demonstration that the probability mass in the long tail is negligibly small in comparison with unity. This posterior justification is also a demonstration of the stability of the solution.

To summarize, the evolution of the distribution of the rolling velocity v ranging from zero to infinity can be described by the Fokker-Planck equation (Eq. 15) with the boundary condition Eq. 17 and, from the definition, the normalization condition. With any appropriately prescribed initial condition, this gives a complete mathematical formulation of the stochastic rolling process and its transient evolution.

Stationary distribution of rolling velocity

In a stationary state, the left-hand side of Eq. 15 vanishes. Integrating it twice with respect to v and using the boundary condition Eq. 17 yield the stationary distribution of velocity p_s.

$$p_s(v) = \frac{1}{\beta^\alpha \Gamma(\alpha)} v^{\alpha-1} \exp\left(-\frac{v}{\beta}\right), \tag{18}$$

where $\Gamma(\alpha)$ is the gamma function and, with the use of Eq. 11,

$$\alpha = \frac{\Delta t}{\tau_2}\left(1 + \frac{\sigma_h^2}{\bar{h}^2}\right)^{-1}, \qquad \beta = \frac{\bar{h}}{\Delta t}\left(1 + \frac{\sigma_h^2}{\bar{h}^2}\right). \tag{19}$$

The coefficient in Eq. 18 has been adjusted to normalize p_s. Eq. 18 is called a gamma distribution. The mean of this distribution is

$$\bar{v} \equiv \langle v \rangle_s = \alpha\beta = \frac{\bar{h}}{\tau_2} \tag{20}$$

as given in Eq. 11, and the variance is

$$\sigma_v^2 \equiv \langle\langle v \rangle\rangle_s = \alpha\beta^2 = \frac{\bar{h}^2}{\tau_2}\left(1 + \frac{\sigma_h^2}{\bar{h}^2}\right) \cdot \frac{1}{\Delta t}. \tag{21}$$

Note that the mean velocity is independent of Δt, whereas the variance of moving-averaged cell velocity is inversely proportional to Δt. These facts are useful in interpreting experimental data.

VELOCITY VARIATION DUE TO THE HETEROGENEITY AMONG CELLS

The stochastic model of cell rolling developed above is for an ensemble of identical cells; the variation of cell velocities in such a homogeneous population is due to the temporal fluctuation of velocities of each cell as a function of time, rather than the heterogeneity among cells.

In reality, however, the variation in the experimentally measured rolling velocities is the consequence of both the temporal fluctuation of the velocity of any particular cell and the heterogeneity among cells. Therefore, to extract a maximum of information from the experimentally determined rolling velocities, we need to separate the contributions of the temporal fluctuations and the cell heterogeneity.

Note that the magnitude of temporal fluctuation within a homogeneous population of cells is a function of the time window Δt, as indicated in Eq. 21, whereas the heterogeneity of the cell population is a concept that is independent of Δt. To formulate these ideas quantitatively, the rolling velocity of a given cell in a stationary state is expressed as

$$v_i = \bar{v}_i + \tilde{v}_i, \tag{22}$$

where the subscript i is the index of the cell, the overbar indicates long-term time average, and the tilde indicates temporal fluctuation. The population average of rolling velocities is defined as

$$\bar{v} \equiv \frac{1}{N}\sum_{i=1}^{N} \bar{v}_i, \tag{23}$$

where N is the population size. Since the population average defined here is compatible with the $\bar{v}$ defined for a homogeneous population in the previous section, the same notation is used in the two cases. The heterogeneity of the population can be measured by the variance of the time-averaged velocities

$$\sigma_{cc}^2 \equiv \frac{1}{N}\sum_{i=1}^{N} (\bar{v}_i - \bar{v})^2, \tag{24}$$

where the subscript cc signifies cell-cell variation. It can be shown that $\bar{v}_i$ is not dependent on the choice of time window Δt. Hence, according to Eqs. 23 and 24 both $\bar{v}$ and σ_{cc}^2 are independent of Δt, as they should be.

Constructing an imaginary ensemble I consisting of members that are exact copies of the particular cell i, and assuming ergodicity for the stationary rolling process of cells in the ensemble I, we have

$$\bar{v}_i = \langle v_i \rangle_I, \qquad \langle \tilde{v}_i \rangle_I = 0, \tag{25a,b}$$

in which $\langle\ \rangle_I$ denotes the average value obtained over the ensemble I. The stochastic model developed in the previous section is applicable to the ensemble I. In particular, from Eq. 21, we have

$$\sigma_i^2 \equiv \langle (v_i - \bar{v}_i)^2 \rangle_I = \frac{\langle h \rangle_I^2}{\langle t_2 \rangle_I}\left(1 + \frac{\langle\langle h \rangle\rangle_I}{\langle h \rangle_I^2}\right) \cdot \frac{1}{\Delta t}, \tag{26}$$

where σ_i^2 is the velocity variance of cell i due to the temporal fluctuation. Let σ_{fl}^2, where the subscript fl signifies fluctuation, denote the population average of σ_i^2. As defined in the previous section, let $\bar{h}$ and σ_h^2 denote, respectively, the population average and variance of step size h, and τ_2 the population average of t_2. Based on Eq. 26, as a zeroth order of approximation we have

$$\sigma_{fl}^2 \approx \frac{\bar{h}^2}{\tau_2}\left(1 + \frac{\sigma_h^2}{\bar{h}^2}\right) \cdot \frac{1}{\Delta t}. \tag{27}$$

The cell velocity v obtained from a single measurement is a random variable. The uncertainty about the velocity arises from the uncertainty about the cell identity and the uncertainty about the temporal fluctuation

$$v = \bar{v}_j + \tilde{v}_j. \tag{28}$$

Here we use j instead of i as the index of cell to emphasize that the cell identity is not specified. Note that in Eq. 22, the cell identity i is assumed to be given and $\bar{v}_i$ is therefore specified; the only uncertainty about v_i is from the temporal fluctuation $\tilde{v}_i$. In contrast, $\bar{v}_j$ in Eq. 28 is a random variable, and so is the temporal fluctuation $\tilde{v}_j$. Let $\langle\ \rangle$ indicate an average over the whole heterogeneous cell population. Then,

$$\langle v \rangle \equiv \frac{1}{N} \sum_{j=1}^{N} (\bar{v}_j + \tilde{v}_j) = \bar{v} + \langle \tilde{v}_j \rangle, \tag{29}$$

where Eq. 23 is used.

When the population size N is large, and the motions of different cells are statistically independent, it is reasonable to assume

$$\langle \tilde{v}_j \rangle = 0. \tag{30}$$

Then $\langle v \rangle = \bar{v}$, where $\bar{v}$ is defined by Eq. 23. Let σ_v^2 be the variance of the cell velocity v given in Eq. 28:

$$\sigma_v^2 \equiv \langle (v - \bar{v})^2 \rangle. \tag{31}$$

Substituting Eq. 28 into Eq. 31 and using Eq. 30 yields

$$\sigma_v^2 = \langle (\bar{v}_j - \bar{v})^2 \rangle + \langle \tilde{v}_j^2 \rangle + 2\langle \bar{v}_j \tilde{v}_j \rangle. \tag{32}$$

According to Eq. 24, the first term on the right-hand side of Eq. 32 is the variance of the time-averaged velocities σ_{cc}^2 due to the heterogeneity among cells. The second term, with the help of Eq. 30, can be identified as σ_{fl}^2, the population average of σ_i^2, signifying the contribution due to temporal fluctuation. Based on the same conditions used in Eq. 30, we assume that the last term is zero (this assumption and Eq. 30 are asymptotically true when $N \to \infty$). Then,

$$\sigma_v^2 = \sigma_{cc}^2 + \sigma_{fl}^2. \tag{33}$$

Inserting Eqs. 24 and 27 into Eq. 33 and multiplying both sides by Δt produces

$$\sigma_v^2 \times \Delta t = \frac{\bar{h}^2}{\tau_2}\left(1 + \frac{\sigma_h^2}{\bar{h}^2}\right) + \sigma_{cc}^2 \times \Delta t. \tag{34}$$

Eq. 34 predicts that when the product of the variance of measured velocities and the time window Δt is plotted against Δt, the data points should fall around a straight line. The intercept of the line is a function of the step size h and waiting time τ_2. The slope of the line gives the variance of the time-averaged cell velocities due to cell heterogeneity.

The mean of the measured cell velocities $\bar{v}$ can be related to the molecular level events as given in Eq. 20. Although Eq. 20 is derived for a stationary ergodic rolling process of a homogeneous population of cells, it should be a good approximation for $\bar{v}$ when the population size is large enough, even if the population is heterogeneous.

The spatial distribution of ligands on a substratum surface is uniform in well-controlled in vitro experiments when measured on a scale much greater than the cell dimension, but randomly changes from point to point on a scale comparable to or smaller than the cell dimension. The macroscopic uniformity of ligand distribution enables the rolling cells to reach a stationary state, at which the statistics of the rolling velocities are time independent. On the other hand, the microscopic variation is experienced by rolling cells as fluctuations along the surface and thus contributes to the temporal fluctuation of rolling velocity σ_{fl}. The heterogeneity of substrata contributes to σ_{cc} and cannot be differentiated from the heterogeneity of rolling cells by using Eq. 34.

For in vitro experiments, the heterogeneity of substrata can be minimized and neglected, and hence σ_{cc} obtained by using Eq. 34 is a measure of the heterogeneity among the rolling cells. For in vivo cell rolling, individual venules may be quite different from each other; in this case σ_{cc} obtained by using Eq. 34 reflects the combination of effects due to the heterogeneity of rolling cells and that of venules. The effects of other relevant surface properties (such as the surface geometry) of the substrata on the velocity variance of rolling cells are similar to those due to the ligand distribution.

COMPARISON TO EXPERIMENTS

For a homogeneous population of rolling cells, the two parameters in the stationary velocity distribution Eq. 18 are directly related to the step size h and waiting time τ_2 by Eq. 19. These parameters can also be computed from the mean and variance of the experimentally determined rolling velocities:

$$\alpha = \frac{(\text{mean velocity})^2}{\text{velocity variance}} = \frac{\bar{v}^2}{\sigma_v^2},$$
$$\beta = \frac{\text{velocity variance}}{\text{mean velocity}} = \frac{\sigma_v^2}{\bar{v}} \tag{35}$$

Here $\sigma_v^2 = \sigma_{fl}^2$ because $\sigma_{cc}^2 = 0$ for a homogeneous population.

The stochastic model predicts that the distribution of the experimentally determined rolling velocities depends on the time window Δt used in calculating velocities. This is verified by experiments of neutrophils rolling on an E-selectin-coated surface and/or IL-1β-stimulated human umbilical vein endothelial cells (HUVECs), which express E-selectin (data not shown here). Fig. 3 shows the effect of varying Δt on the change of velocity distribution for a given set of data, i.e., with all the other quantities at the right-hand side of Eq. 19 being fixed. It can be seen that the velocity distribution

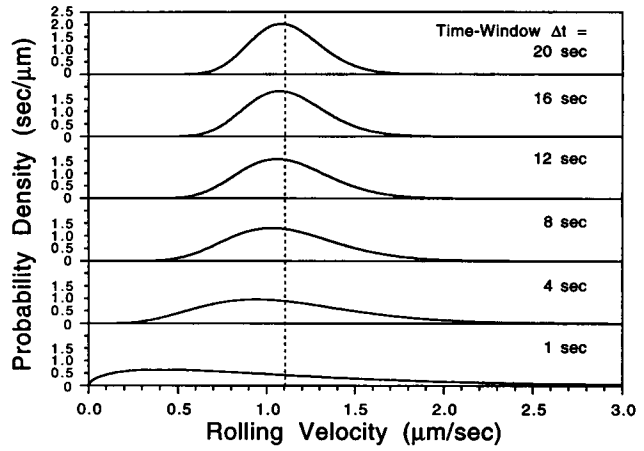

FIGURE 3 Dependency of velocity distribution on the time window Δt. Continuous curves are theoretical velocity distributions generated by Eqs. 18 and 19, with parameters intrinsic to the rolling process being fixed: $\bar{h} = 0.52$ μm, $\tau_2 = 0.47$ s, and $\sigma_h/\bar{h} = 0.5$, as estimated from data in Fig. 6 for neutrophils rolling on an E-selectin-coated surface. The dashed line indicates the mean of rolling velocities, which is independent of time window Δt.

becomes narrower when the time window Δt increases, indicating the smoothing effect of a large Δt on the temporal fluctuation of individual cells.

Table 1 lists the results of the use of the present approach to analyze the experimental data reported by Jones et al. (1993) on neutrophils rolling on histamine-stimulated HUVECs, which express P-selectin. The first four columns are their reported values of means and variances of the rolling velocities under various wall shear stresses (using $\Delta t = 4$ s), as shown in their table 2. The last two columns show the corresponding values of α and β computed from their data by using Eq. 35. Fig. 4 shows the theoretical distributions of the probability densities of the rolling velocity computed from Eq. 18 by using the α and β values given in Table 1 and the experimental distributions (bar graphs) given by Jones et al. (1993). The computed distributions agree very well with the experimentally determined frequency histograms of rolling velocities. Fig. 5 shows the comparison of the same theoretical and experimental data as presented in Fig. 4, but they are plotted in terms of the cumulative frequencies. Assuming that the cell populations are homogeneous and using $\Delta t = 4$ s as in the experiments of Jones et al. (1993), we can estimate the step sizes and waiting times by using Eq. 19. The results are $h \approx 6.1$ μm and $\tau_2 \approx 0.92$ s for the case of the lowest shear stress and $h \approx 16$ μm and $\tau_2 \approx 0.53$ s for the case of the highest shear stress, in which $1 + (\sigma_h^2/\bar{h}^2)$ has been assumed to be 1.25. Both the step sizes and waiting times are probably overestimated in this computation because the heterogeneity of the real population, which would contribute to the spread of the experimentally determined velocities. The effect of the population heterogeneity on the above estimation is positively correlated to the ratio of $\Delta t/\tau_2$. The tendency of better agreement between the model and experiment for the cases of lower wall shear stresses (Fig. 4) supports this analysis, because the lower the wall shear stress (and hence the mean rolling velocity), the smaller is the ratio $\Delta t/\tau_2$ for a given Δt, i.e., heterogeneity of cells has less effect.

It is difficult to eliminate the effects of the heterogeneity of a population of real cells. However, our model provides a practical way to separate the contribution to the velocity variance of temporal fluctuation from that of the heterogeneity among cells by varying the time window Δt used in analyzing experimental data. Fig. 6 shows an example. The data points are of human neutrophils rolling on an E-selectin-coated polystyrene slide observed in a linear shear stress flow chamber (Usami et al., 1993) at a location where the shear stress is 1.2 dyn/cm^2. E-selectin-coated polystyrene slides were prepared at room temperature by the incubation of 2.5 μg/ml soluble E-selectin overnight, followed by 1 h of blocking with 1% bovine serum albumin. The instantaneous positions of 19 rolling cells were determined from the recorded video images at a rate of 30/s over a period of 20 s. For every chosen time window Δt, the 20-s period was sectioned into equal time intervals Δt. The cell velocities were computed by using Eq. 4 from the cell displacement over every such time interval for every cell. The mean and variance of the cell velocities were computed for the chosen time window Δt. The mean was found to be independent of the time window Δt, as it should be according to Eq. 20. However, when Δt increased, the variance of cell velocities decreased (Fig. 6 *A*). Eq. 34 predicted that the product of the velocity variance and the time window Δt is linearly dependent on Δt. As shown in Fig. 6 *B*, when

TABLE 1 Summary of statistics for the velocity distribution of neutrophils rolling on histamine-stimulated HUVECs at various shear stresses*

Wall shear stress (dyn/cm^2)	No. of neutrophils	Mean rolling velocity (μm/s)	SD (μm/s)	α	β (μm/s)
0.31	240	6.63	3.55	3.488	1.901
0.62	180	8.81	4.34	4.121	2.138
1.23	361	12.80	7.02	3.325	3.850
2.47	377	16.32	7.63	4.575	3.567
4.94	294	23.21	9.17	6.406	3.623
7.64	181	29.87	12.1	6.094	4.902

* Experimental data in the first four columns are those reported by Jones et al. (1993). The parameters α and β were computed from these data by using Eq. 35.

plotted in accordance with Eq. 34, the data points indeed are close to a straight line. From the slope of the linear regression of the data points shown in Fig. 6 *B*, the variance of the time-averaged velocities is obtained as $\sigma_{cc}^2 = 0.12\ (\mu m/s)^2$. The mean of the rolling velocities was $\bar{v} = 1.1\ \mu m/s$. A quantitative measure of the heterogeneity among the individual cells is the coefficient of variation for the time-averaged velocities: $\sigma_{cc}/\bar{v} = 0.31$. Ideally, if Δt were large enough, the temporal fluctuation in rolling velocities would be averaged out and the variance of rolling velocities σ_v^2 would approach the limit σ_{cc}^2. As shown in Fig. 6 *A*, at $\Delta t = 20$ s, $\sigma_v^2 = 0.15\ (\mu m/s)^2$, which was still 25% greater than the σ_{cc}^2 given above by Eq. 34. In this case, to estimate σ_{cc}^2 directly from the rolling velocities determined experimentally with a large time window Δt, we would have to use $\Delta t > 120$ s to ensure an error within 5%.

The intercept of the linear regression was $0.72\ \mu m^2/s$ (Fig. 6 *B*). From this and the mean of the rolling velocities, and with the use of Eqs. 20 and 34, we find $\bar{h} = 0.65\ \mu m \times (1 + \sigma_h^2/\bar{h}^2)^{-1}$ and $\tau_2 = 0.59\ s \times (1 + \sigma_h^2/\bar{h}^2)^{-1}$. Assuming that $\sigma_h/\bar{h}$ (the coefficient of variation for the step size h) was 0.5, we obtained an estimation of the mean of the step size $\bar{h} = 0.52\ \mu m$, and the mean of the time intervals between successive jumps (the waiting-time) $\tau_2 = 0.47$ s.

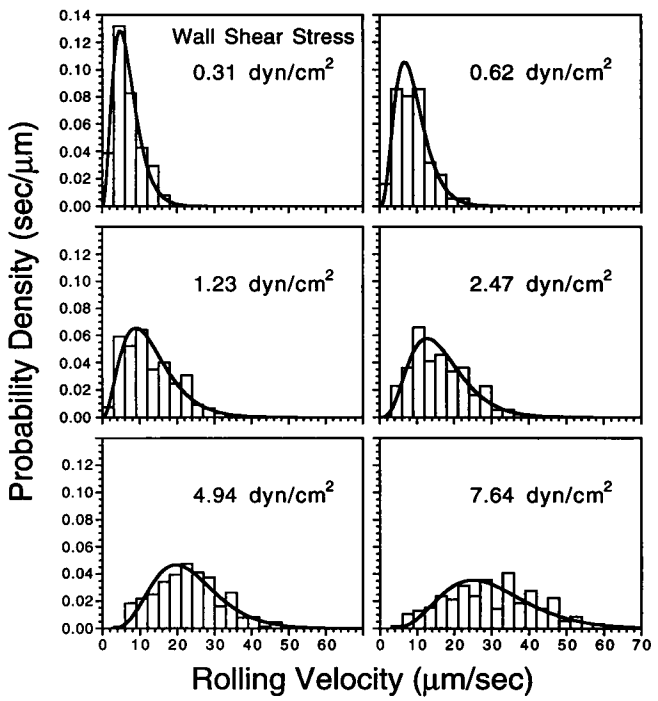

FIGURE 4 Comparison between the theoretical distribution computed using Eq. 18 (continuous curves) and the experimental data (bar graphs) on neutrophil rolling on histamine-stimulated HUVECs (which present P-selectins) at various wall shear stresses. The velocity histograms are reproduced from Fig. 8 of Jones et al. (1993). The curves are theoretical distributions with means and variances set equal to those of the experimental data as listed in Table 1. The deviations of the theoretical and experimental distributions at high wall shear stresses reflect the influence of the population heterogeneity, as discussed in the text.

DISCUSSION

The above analysis constitutes a mathematical model for the stochastic motion of leukocytes rolling in a shear flow. The model gives the stationary distribution of rolling velocities in analytical form for a homogeneous population of leukocytes. Furthermore, it allows the separation of contributions from temporal fluctuation in rolling velocities and from population heterogeneity among cells to the variance of experimentally determined rolling velocities. The mean of the rolling velocities and the velocity variance due to temporal fluctuation are related to the quantities characterizing the distribution and the release rate of the clusters of molecular bonds as given in Eqs. 20 and 21.

The rolling velocity in our model is defined as the moving average of the instantaneous velocities over a time window Δt. There are two reasons for doing this. First, this is consistent with the experimental method used to determine the velocities of rolling cells. The time window used in an experiment is usually much greater than the waiting time τ_2. Therefore, the measured velocities cannot be considered as instantaneous velocities. Our model predicts that the distribution of rolling velocities obtained from experimental measurements will be influenced by the choice of Δt (Fig. 3). Only when a consistent time window is used both in experiment and in modeling, can a theoretical distribution, e.g., the one given here or that generated by computer simulation (Hammer and Apte, 1992), be directly compared to a velocity distribution determined experimentally. This is also pertinent when comparing the variances of rolling velocities given by the mathematical model to those determined experimentally, or when comparing the distributions or variances of rolling velocities acquired under different experimental conditions. Hence, any data on rolling velocities should explicitly include the time window Δt used in computing the velocities from the raw experimental data.

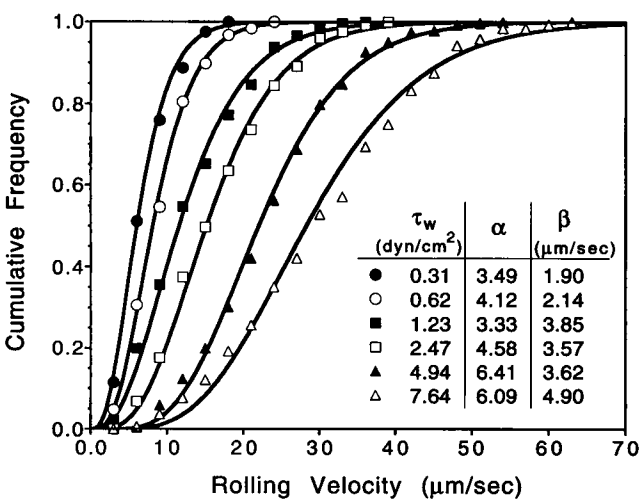

FIGURE 5 Comparison between theoretical (curves) and experimental (points) distributions in Fig. 4 expressed in terms of cumulative frequencies. τ_w is wall shear stress; α and β are model parameters in the theoretical distribution (Eq. 18).

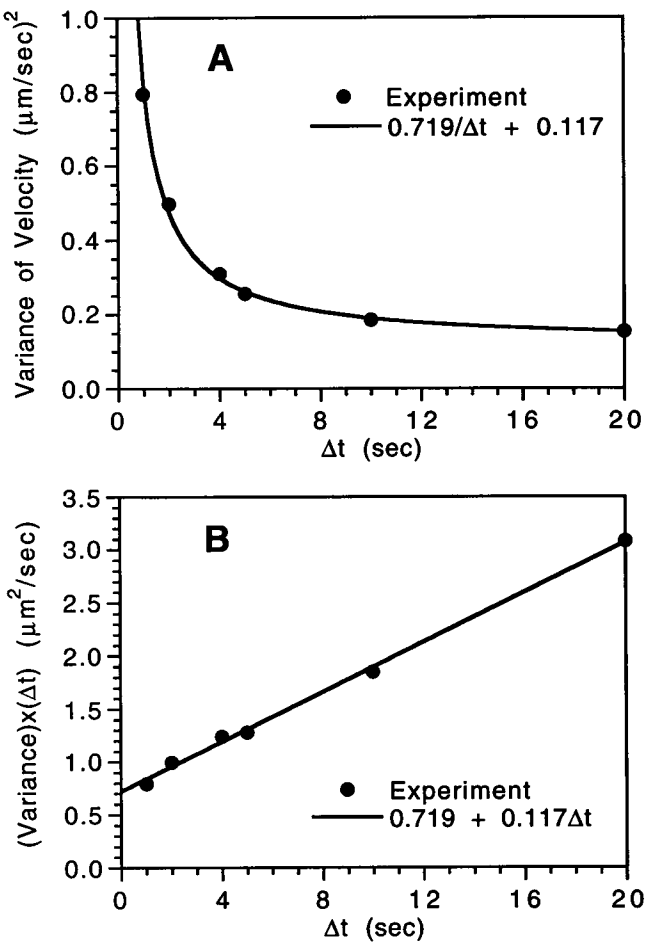

FIGURE 6 Comparison between the model prediction (Eq. 34) and experimental data on neutrophil rolling on E-selectin-coated surface at a wall shear stress of 1.2 dyn/cm^2. All points are computed from the same set of raw data on the positions of 19 rolling cells over a 20-s period. The different data points were obtained by using different time windows Δt in computing the moving-average velocity as defined in Eq. 4. The ensemble average velocity is 1.1 dyn/cm^2, which is independent of Δt. (*A*) The velocity variance is a decreasing function of increasing time window Δt. The variance approaches a nonzero limit for large Δt, reflecting the heterogeneity among cells. (*B*) linear regression of the data replotted in coordinates suggested by Eq. 34. The nonzero intercept is a result of temporal fluctuation of the leukocyte motion. The average values of step size and waiting time can be estimated from the intercept and the average velocity to be, respectively, $\bar{h} = 0.52$ μm and $\tau_2 = 0.47$ s, with the assumption that the coefficient of variation for the step size $\sigma_h/\bar{h}$ is 0.5. The slope is the variance of the long-term time averages of the rolling velocities of individual cells. It is a measure of cell heterogeneity.

The second reason for introducing the moving-average velocity is to ensure that the velocity under consideration is smooth enough to be modeled as a diffusion process in a Fokker-Planck type approach to studying the temporal fluctuation of the rolling motion. This approach is appropriate when the displacement of a rolling cell is approximately a stepwise function of time, as discussed above. The instantaneous rolling velocity of the cell is then a series of sharp peaks of random heights on the order of $\bar{h}/\tau_1$ and width τ_1, occurring successively at random time intervals on the order of τ_2, where $\tau_1 \ll \tau_2$ because of the fact that rolling velocity is much smaller than the velocity of a nonadherent cell freely moving immediately adjacent to the substratum surface. The extent of the smoothing of the instantaneous rolling velocities by the use of the moving average is determined by the dimensionless ratio $\Delta t/\tau_2$. The larger is this ratio, the smoother is the rolling velocity. To ensure that the rolling velocity is smooth enough to be approximated as a diffusion process requires $\Delta t/\tau_2$ to be large enough, which is usually satisfied in experiments, as mentioned previously. When this ratio approaches infinity, the temporal fluctuations in rolling velocities are completely smoothed out, and consequently the variability of the measured rolling velocities is then purely a reflection of the population heterogeneity of the cells, which can be characterized by σ_{cc}^2 defined in Eq. 24.

As a verification of the model, we compared the theoretical distribution of Eq. 18 to the velocity histograms of neutrophils rolling on histamine-stimulated endothelial cells at various wall shear stresses (Jones et al., 1993), as shown in Figs. 4 and 5. The parameters in the theoretical distribution are determined by equating its mean and variance to that of experimental velocities. Note that the theoretical distribution of Eq. 18 is derived for the stationary rolling motion of a homogeneous population of cells. In the experiments of Jones et al. (1993), "neutrophils that remain stationary for the 4 s of acquisition (typically approximately 5%) are excluded, since this population of neutrophils may be activated and may be utilizing different binding mechanisms." This greatly reduces the heterogeneity of the population of the rolling cells by removing the apparent outliers. "Also, neutrophils that either begin rolling on the endothelium or reenter the free stream during the acquisition period are excluded." Thus, the rolling motion of the remaining cells can be considered to be stationary. Hence, both homogeneity and stationarity are approximately satisfied. Indeed, Figs. 4 and 5 show excellent agreement between the theoretical distribution obtained by using Eq. 18 and the histograms of experimental rolling velocities.

As discussed in the previous section, Figs. 4 and 5 also show some influence of the population heterogeneity on the histograms of measured rolling velocities according to the explanation provided by our model. The influence of the population heterogeneity can also be seen by comparing the kurtosis computed from the experimental data to the kurtosis expected from the distribution of Eq. 18. Kurtosis is a dimensionless number that measures the peakedness or flatness of a distribution relative to the normal distribution. In table 2 of Jones et al. (1993), kurtosis is negative except in one of the six cases, indicating that the distribution of rolling velocities for the real cells is flatter than a normal distribution. The kurtosis of the theoretical distribution (Eq. 18) is always positive. This discrepancy in kurtosis may be explained by the heterogeneity of the cell population. In other words, it is an indication that the data are "contaminated" by population heterogeneity among the cells. We expect that the distribution of the long-term time averages

of rolling velocities (i.e., the distribution of $\bar{v}_j$ in Eq. 28, which reflects the heterogeneity of the cell population) is quite flat, and therefore its kurtosis is negative. The "contamination" of an otherwise more peaked distribution by the flatly distributed $\bar{v}_j$ due to heterogeneity smears the peak, resulting in a negative kurtosis for the overall distribution of measured velocities. It should be kept in mind that the kurtosis is a fourth moment of the velocity distribution. When estimated from a sample of a finite size, its numerical value is far less reliable than the estimates of lower moments such as the mean and variance. Hence, the discussion here is only qualitative in regard to how the kurtosis reflects the influence of heterogeneity on velocity distribution.

To completely circumvent the effects of heterogeneity of a cell population on rolling velocity distribution is essentially impossible in experiments. Overestimations of the step size and waiting time would occur if the influence of the population heterogeneity on the velocity variability is not isolated and removed before using Eqs. 20 and 21. The velocity variability due to population heterogeneity itself may be of interest, because it may help us to obtain useful knowledge such as the distribution of adhesion receptor numbers or age among the cells. Our model provides a practical method of accomplishing this isolation, as exemplified in the previous section by using data on neutrophils rolling on an E-selectin-coated surface. Again, the agreement between the model prediction (Eq. 34) and available experimental data is quite satisfactory, as shown in Fig. 6. The waiting time τ_2 (i.e., the average arrest duration) in this case is estimated to be 0.47 s, which is positively correlated to the lifetime of the stressed molecular bonds at the rearmost microvillus tip. A comparison of this waiting time to the median duration of cell arrests (2.43 s) obtained by Kaplanski et al. (1993) for neutrophils moving over E-selectin-expressing HUVECs in a flow of extremely small shear rate is of interest from a molecular level viewpoint. In their experiments, the cells are believed to be arrested most often by one bond; and the fluid force imparted to a cell is much weaker than the mechanical strength of a standard receptor-ligand bond (Kaplanski et al., 1993). This weak stress applied to the bond makes the lifetime of the bond about 1 million times shorter than the lifetime expected for a stress-free bond (Kaplanski et al., 1993). In our case, the fluid drag on the cell is about 23 times higher than in Kaplanski's data. Although there may be more than one bond involved in the rolling adhesion, the stress on an individual bond at the rearmost microvillus in our case is most likely higher than in their case. The average lifetime of a stressed bond in our case ($<\tau_2 \sim 0.5$ s) is shorter than in Kaplanski's cases but still is of the same order of magnitude. The suggestion of this comparison is that the lifetime of E-selectin bonds decreases catastrophically when they are stretched by a weak force, and that the lifetime of the bond reaches a plateau with respect to the applied stress before the stress approaches a critical value that will mechanically rupture the bond immediately.

The dependence of the lifetime (or the apparent dissociation rate) of E-selectin bonds on the applied force provides a basis for analysis of the mechanics of cell rolling. For individual bonds, the transition from the steep dependence of the bond lifetime on the applied force to the much slower second phase could be very sharp. The waiting time t_2 is influenced by the number of bonds in the rearmost clusters. Presence of multiple bonds and the randomness of the bond number in the rearmost clusters blurs the transition of τ_2 as a function of fluid force from the fast phase to the slow phase. In any case, as the fluid shear stress increases, the mean rolling velocity of cells increases relatively rapidly at the beginning and then becomes flatter at larger fluid shear stress. This behavior of mean velocity as a function of applied fluid shear stress has been observed for both P-selectin- and E-selectin-mediated cell rolling at various surface densities of selectins on substratum (Lawrence and Springer, 1991, 1993; Jones et al., 1993).

The surface density of ligands on the substratum affects the rolling velocity of given cells by influencing both the step size h and the waiting time t_2. Lowering the ligand surface density decreases the chance of the receptors at microvillus tips to react with the ligands and make bonds. For a microvillus possessing very few receptors, the probability of no bond formation increases. This increases the mean step size $\bar{h}$. Meanwhile, for the microvilli making bonds, the average number of bonds per microvillus decreases. This increases the force on individual bonds in the rearmost clusters. Both the increasing force on individual bonds and the decreasing number of bonds accelerate the release rate of the rearmost bond cluster and thus shorten the average waiting time τ_2. According to Eqs. 20 and 21, the theory predicts that larger $\bar{h}$ and smaller τ_2 will increase both the mean and the variance of the rolling velocity.

At very low surface density of ligands on the substratum, the chance for receptors on a microvillus tip to meet a ligand on the substratum surface may decrease to a level such that the probability of having more than one cluster of bonds is practically zero. Then it is likely that only one cluster (most probably consisting of a single bond) exists throughout the stationary period. The release of this bond cluster then frees the cell completely and the cell moves at its free-streaming velocity until the formation of new bonds. During the free-streaming period, the motion of a spherical cell is a combination of rolling and sliding (Goldman et al., 1967). What occurs is no longer cell rolling. Experimentally, one observes cells moving at free-streaming velocity with occasional arrests. Because of the small chance of bringing the receptor and ligand together for a reaction, the nonzero velocity period (t_1 in Fig. 2) may last for a long time and the condition $\tau_1 \ll \tau_2$ may not be satisfied. Hence, the present form of the theory may not be applicable to this case.

The effect of applied stress on the lifetime (or the dissociation rate) of receptor-ligand bonds has been a focus of interest in recent discussions of cell adhesion. Although novel experimental methods have been developed recently to determine the force needed to rapidly rupture an individ-

ual receptor-ligand bond (Tha et al., 1986; Evans et al., 1991; Leckband et al., 1992; Florin et al., 1994; Moy et al., 1994), direct measurement of the relationship of bond lifetime to stress on individual bonds is still missing. In previous models of cell adhesion (Bell, 1978; Dembo et al., 1988; Hammer and Apte, 1992; Tözeren and Ley, 1992), a functional form of this relationship is assumed. Then the values of the parameters, or their ranges, are searched by comparing the mean cellular velocity generated by the models to experimental data. The model presented here points to a much more direct and definite way of determining the lifetime-stress relationship of cells rolling in their in vivo environment by providing a simple method of estimating the waiting time τ_2 from the data of cell rolling. To complete this computation it is necessary to have data on how, in a statistical sense, the fluid force distributes over the individual molecular bonds. This issue is the focus of our future investigations.

We are grateful to Professor Martin Ostoja-Starzewski for useful discussion on stochastic methods.

This research was partially supported by USPHS research grant from the National Heart Lung and Blood Institute HL43026.

REFERENCES

Abbassi, O., T. K. Kishimoto, L. V. McIntire, D. C. Anderson, and C. W. Smith. 1993. E-selectin supports neutrophil rolling in vitro under conditions of flow. *J. Clin. Invest.* 92:2719–2730.

Bell, G. I. 1978. Models for the specific adhesion of cells to cells. *Science.* 200:618–627.

Bevilacqua, M. P., and R. M. Nelson. 1993. Selectins. *J. Clin. Invest.* 91:379–387.

Borregaard, N., L. Kjeldsen, H. Sengelov, M. S. Diamond, T. A. Springer, H. C. Anderson, T. K. Kishimoto, and D. F. Bainton. 1994. Changes in subcellular localization and surface expression of L-selectin, alkaline phosphatase, and Mac-1 in human neutrophils during stimulation with inflammatory mediators. *J. Leukoc. Biol.* 56:80–87.

Dembo, M., D. C. Torney, K. Saxman, and D. Hammer. 1988. The reaction-limited kinetics of membrane-to-surface adhesion and detachment. *Proc. R. Soc. Lond. B. Biol. Sci.* 234:55–83.

Erlandsen, S. L., S. R. Hasslen, and R. D. Nelson. 1993. Detection and spatial distribution of the beta 2 integrin (Mac-1) and L-selectin (LECAM-1) adherence receptors on human neutrophils by high-resolution field emission SEM. *J. Histochem. Cytochem.* 41:327–333.

Etzioni, A., J. M. Harlan, S. Pollack, L. M. Phillips, R. Gershoni-Baruch, and J. C. Paulson. 1993. Leukocyte adhesion deficiency (LAD) II: a new adhesion defect due to absence of sialyl Lewis X, the ligand for selectins. *Immunodeficiency.* 4:307–308.

Evans, E., D. Berk, and A. Leung. 1991. Detachment of agglutinin-bonded red blood cells. I. Forces to rupture molecular-point attachments. *Biophys. J.* 59:838–848.

Fiebig, E., K. Ley, and K. E. Arfors. 1991. Rapid leukocyte accumulation by "spontaneous" rolling and adhesion in the exteriorized rabbit mesentery. *Int. J. Microcirc. Clin. Exp.* 10:127–144.

Florin, E. L., V. T. Moy, and H. E. Gaub. 1994. Adhesion forces between individual ligand-receptor pairs. *Science.* 264:415–417.

Goetz, D. J., M. E. el-Sabban, B. U. Pauli, and D. A. Hammer. 1994. Dynamics of neutrophil rolling over stimulated endothelium in vitro. *Biophys. J.* 66:2202–2209.

Goldman, A. J., R. G. Cox, and H. Brenner. 1967. Slow viscous motion of a sphere parallel to a plane wall—II Couette flow. *Chem. Eng. Sci.* 22:653–660.

Hammer, D. A., and S. M. Apte. 1992. Simulation of cell rolling and adhesion on surfaces in shear flow: general results and analysis of selectin-mediated neutrophil adhesion. *Biophys. J.* 63:35–57.

Harlan, J. M. 1993. Leukocyte adhesion deficiency syndrome: insights into the molecular basis of leukocyte emigration. *Clin. Immunol. Immunopathol.* 67:S16–S24.

Jones, D. A., O. Abbassi, L. V. McIntire, R. P. McEver, and C. W. Smith. 1993. P-selectin mediates neutrophil rolling on histamine-stimulated endothelial cells. *Biophys. J.* 65:1560–1569.

Kaplanski, G., C. Farnarier, O. Tissot, A. Pierres, A. M. Benoliel, M. C. Alessi, S. Kaplanski, and P. Bongrand. 1993. Granulocyte-endothelium initial adhesion. Analysis of transient binding events mediated by E-selectin in a laminar shear flow. (see comments) *Biophys. J.* 64: 1922–1933.

Lasky, L. A. 1992. Selectins: interpreters of cell-specific carbohydrate information during inflammation. *Science.* 258:964–969.

Lawrence, M. B., and T. A. Springer. 1991. Leukocytes roll on a selectin at physiologic flow rates: distinction from and prerequisite for adhesion through integrins. *Cell.* 65:859–873.

Lawrence, M. B., and T. A. Springer. 1993. Neutrophils roll on E-selectin. *J. Immunol.* 151:6338–6346.

Leckband, D. E., J. N. Israelachvili, F. J. Schmitt, and W. Knoll. 1992. Long-range attraction and molecular rearrangements in receptor-ligand interactions. *Science.* 255:1419–1421.

Ley, K. 1993. Molecular mechanisms of leucocyte rolling and adhesion to microvascular endothelium. *Eur. Heart J.* 14(suppl. I):68–73.

Lipowsky, H. H., D. Riedel, and G. S. Shi. 1991. In vivo mechanical properties of leukocytes during adhesion to venular endothelium. *Biorheology.* 28:53–64.

Lorant, D. E., M. K. Topham, R. E. Whatley, R. P. McEver, T. M. McIntyre, S. M. Prescott, and G. A. Zimmerman. 1993. Inflammatory roles of P-selectin. *J. Clin. Invest.* 92:559–570.

McEver, R. P. 1994. Selectins. *Curr. Opin. Immunol.* 6:75–84.

Moy, V. T., E. L. Florin, and H. E. Gaub. 1994. Intermolecular forces and energies between ligands and receptors. *Science.* 266:257–261.

Picker, L. J., R. A. Warnock, A. R. Burns, C. M. Doerschuk, E. L. Berg, and E. C. Butcher. 1991. The neutrophil selectin LECAM-1 presents carbohydrate ligands to the vascular selectins ELAM-1 and GMP-140. (Published erratum appears in *Cell* 1991, 67(6):1267) *Cell.* 66:921–933.

Schmid-Schönbein, G. W., R. Skalak, S. I. Simon, and R. L. Engler. 1987. The interaction between leukocytes and endothelium in vivo. *Ann. NY Acad. Sci.* 516:348–361.

Springer, T. A. 1990. Adhesion receptors of the immune system. *Nature.* 346:425–434.

Tha, S. P., J. Shuster, and H. L. Goldsmith. 1986. Interaction forces between red cells agglutinated by antibody. II. Measurement of hydrodynamic force of breakup. *Biophys. J.* 50:1117–1126.

Tözeren, A., and K. Ley. 1992. How do selectins mediate leukocyte rolling in venules? *Biophys. J.* 63:700–709.

Usami, S., H. H. Chen, Y. Zhao, S. Chien, and R. Skalak. 1993. Design and construction of a linear shear stress flow chamber. *Ann. Biomed. Eng.* 21:77–83.

Ushiyama, S., T. M. Laue, K. L. Moore, H. P. Erickson, and R. P. McEver. 1993. Structural and functional characterization of monomeric soluble P-selectin and comparison with membrane P-selectin. *J. Biol. Chem.* 268:15229–15237.

von Andrian, U. H., E. M. Berger, L. Ramezani, J. D. Chambers, H. D. Ochs, J. M. Harlan, J. C. Paulson, A. Etzioni, and K. E. Arfors. 1993. In vivo behavior of neutrophils from two patients with distinct inherited leukocyte adhesion deficiency syndromes. *J. Clin. Invest.* 91: 2893–2897.

von Andrian, U. H., J. D. Chambers, L. M. McEvoy, R. F. Bargatze, K. E. Arfors, and E. C. Butcher. 1991. Two-step model of leukocyte-endothelial cell interaction in inflammation: distinct roles for LECAM-1 and the leukocyte beta 2 integrins in vivo. *Proc. Natl. Acad. Sci. USA.* 88:7538–7542.

Welply, J. K., J. L. Keene, J. J. Schmuke, and S. C. Howard. 1994. Selectins as potential targets of therapeutic intervention in inflammatory diseases. *Biochim. Biophys. Acta.* 1197:215–226.